Geochemical Perspectives Letters

Sulfur and mercury MIF suggest volcanic contributions to Earth's atmosphere at 2.7 Ga

A.L. Zerkle, M.W. Claire, T. Di Rocco, N.V. Grassineau, E.G. Nisbet, R. Sun, R. Yin

Supplementary Information

The Supplementary Information includes:

- Materials and Methods
- Tables S-1 to S-3
- Figures S-1 and S-2
- Supplementary Information References

Materials and Methods

Our samples were collected from three drill cores through the ~2.7 Ga Manjeri Formation (Fm) of the Belingwe Greenstone Belt in Zimbabwe (Fig. S-1). This section of the Manjeri Fm records a marine transgression from the intertidal facies of the Spring Valley member and subtidal Shavi member to the exceptionally well-preserved shales of the Jimmy member. Sedimentary textures imply that the Jimmy member was deposited in a deeper shelf setting below wave base (Grassineau *et al.*, 2006). Lead-lead isochrons derived from stromatolites of the Manjeri Fm indicate a depositional age of 2.706 ± 0.049 Ga (Bolhar *et al.*, 2002). Overall, the metamorphic grade of the studied succession is remarkably low for rocks of this age, as supported by the preservation of texturally pristine and mineralogically unaltered komatiites (Nisbet *et al.*, 1987). The studied drill cores, NERCMAR, Core A and Core B, were taken from the eastern margin of the Belingwe belt (Fig. S-1, S-2), where the Manjeri Fm unconformably overlies much older gneissic crust. The detailed geological setting and stratigraphy of the NERCMAR drill core, which intersects the entirety of the Manjeri Fm, was described in Grassineau *et al.* (2006). Cores A and B, which recovered extensive sections of the Jimmy member, were described in detail by Yang *et al.* (2019).

Sulfide extractions were performed in the Geobiology Lab at the University of St Andrews using the chromium reduction method, as described previously (Izon *et al.*, 2015). Major sulfur isotope analyses ($\delta^{34}S$) were performed on the resulting silver sulfide (Ag_2S) by Iso-Analytical Laboratories, Cheshire, UK, using standard EA-IRMS techniques, and reported in Yang *et al.* (2019). Minor S isotope analyses were conducted in the gas-source isotope geochemistry laboratory at the University of St Andrews, using a Curie-point pyrolysis sulfur fluorination line, as detailed in Warke *et al.* (2020).

The resulting sulfur isotope ratios ($^{33}S/^{32}S$, $^{34}S/^{32}S$, $^{36}S/^{32}S$) are reported using the standard delta notation (δ) showing per mil (‰) deviations from international standard V-CDT, as follows:

$$\delta^{3X}S\ (‰) = [{}^{3X}S/{}^{32}S_{sample}/{}^{3X}S/{}^{32}S_{V\text{-}CDT} - 1] \times 1000 \quad \text{(Eq. S-1)}$$

where ^{3X}S is ^{33}S, ^{34}S, or ^{36}S. Minor S isotope values are further expressed using $\Delta^{33}S$ and $\Delta^{36}S$ notation, calculated as:

$$\Delta^{33}S\ (‰) = \delta^{33}S - [({}^{34}S/{}^{32}S_{sample}/{}^{34}S/{}^{32}S_{V\text{-}CDT})^{0.515} - 1] \quad \text{(Eq. S-2)}$$

$$\Delta^{36}S\ (‰) = \delta^{36}S - [({}^{34}S/{}^{32}S_{sample}/{}^{34}S/{}^{32}S_{V\text{-}CDT})^{1.90} - 1]. \quad \text{(Eq. S-3)}$$

Long-term reproducibility of this method based on repeat analyses of IAEA-S1 (n = 75) is 0.014‰ for $\Delta^{33}S$ and 0.190‰ for $\Delta^{36}S$.

Total Hg concentrations were determined by the RA-915+ Hg analyzer coupled with the PYRO-915+ attachment (Lumex, Russia), at the Institute of Geochemistry, Chinese Academy of Sciences (IGCAS). Recoveries for standard reference material GSS-5 (n=3) were between 90 and 110 %, and coefficients of variation (triplicate analyses) were < 10 %. A double-stage tube furnace coupled with 5 mL of 40 % acid mixture (HNO3/HCl = 2/1, v/v) was used for preconcentration of Hg for isotope analysis (Deng *et al.*, 2021). The preconcentrated solutions were diluted to 0.5 ng/mL Hg and measured and analysed by Neptune Plus multi-collector inductively coupled plasma mass spectrometer (Thermo Electron Corp, Bremen, Germany) at IGCAS, following a previous method (Yin *et al.*, 2016). Mercury isotopes were expressed following conventional notation (Bergquist and Blum, 2007), such that mass-dependent fractionation (MDF) was expressed as $\delta^{202}Hg$ (in ‰) referenced to the NIST SRM 3133 Hg standard (analyzed before and after each sample):

$$\delta^{202}Hg\ (‰) = [{}^{202}Hg/{}^{198}Hg_{sample}/{}^{202}Hg/{}^{198}Hg_{standard} - 1] \times 1000. \quad \text{(Eq. S-4)}$$

Mass independent fractionation of Hg isotopes is further expressed in permil (‰), using $\Delta^{199}Hg$ and $\Delta^{201}Hg$ notation for odd-number Hg-MIF, and $\Delta^{200}Hg$ notation for even-number Hg-MIF, calculated as:

$$\Delta^{xxx}Hg\ (‰) = \delta^{xxx}Hg - \delta^{202}Hg \times \beta \quad \text{(Eq. S-5)}$$

where β is equal to 0.2520 for ^{199}Hg, 0.5024 for ^{200}Hg, and 0.7520 for ^{201}Hg. NIST-3177 secondary standard solutions, diluted to 0.5 ng/mL Hg with 10% HCl, were measured every 10 samples. The overall average and uncertainty of NIST-3177 and GSS-5 (Table S-3) agree well with previous results (Blum and Bergquist, 2007; Deng *et al.*, 2021). Uncertainties reported in this study (Table S-2) correspond to the larger value of either the measurement uncertainty of replicate digests of GSS-5 or the uncertainty of repeated measurements of UM-Almadén.

Supplementary Tables

Table S-1 Sulfur isotope data for the Manjeri Formation, given in ‰ relative to V-CDT. $\delta^{34}S$ values are as reported in Yang *et al.* (2019). Errors shown (1σ) are for individual measurements.

Sample	Member	Depth (m)	$\delta^{34}S$	$\Delta^{33}S$	1σ	$\Delta^{36}S$	1σ
B1-1	Jimmy	61.5	-10.3	-0.353	0.022	0.440	0.146
B2-1	Jimmy	63.31	-11.2	-0.365	0.012	0.537	0.151
B2-3	Jimmy	65.2	-7.1	0.881	0.023	-0.862	0.312
B2-11	Jimmy	65.35	-6.6	1.183	0.014	-2.486	0.134
B2-15	Jimmy	67.06	-5.5	1.407	0.022	-1.553	0.094
B2-18	Jimmy	68.14	-11.8	1.145	0.008	-1.527	0.091
B2-20	Jimmy	69.16	-8.0	0.381	0.019	-0.034	0.151
B3-02	Jimmy	70.72	-11.1	0.358	0.023	-0.121	0.160
B3-03	Jimmy	71.75	-3.0	0.951	0.029	-0.494	0.178
B3-13	Jimmy	72.5	3.4	2.190	0.014	-2.202	0.117
B3-14	Jimmy	73.15	1.4	2.509	0.023	-2.293	0.181
B3-17	Jimmy	74.74	2.4	2.715	0.020	-2.519	0.138
B4-19	Jimmy	75.58	-18.0	1.690	0.032	-0.631	0.196
B4-9	Jimmy	77.53	3.1	2.634	0.016	-2.493	0.08
B4-12	Jimmy	79.35	3.3	2.826	0.013	-3.372	0.044
B4-15	Jimmy	80.65	4.0	3.188	0.014	-3.130	0.105
B4-07	Jimmy	83.1	4.5	3.024	0.018	-3.102	0.121
B4-20	Jimmy	83.32	3.8	2.930	0.032	-1.956	0.18
B4-08	Jimmy	84.13	-9.3	1.645	0.037	-0.167	0.233
A7-6	Jimmy	102.65	-4.7	0.444	0.008	-0.268	0.105
A7-8	Jimmy	103.85	-7.4	0.469	0.014	-0.556	0.129
A7-7	Jimmy	103	-5.4	0.397	0.009	-0.365	0.150
A8-3	Jimmy	108.58	-1.5	1.124	0.015		
A7-3	Jimmy	104.48	-33.7	-0.169	0.020	1.441	0.179
A8-14	Jimmy	110.41	-2.3	0.497	0.016	-0.463	0.09
A7-4	Jimmy	105.53	-2.1	1.266	0.015	-1.267	0.161
A8-16	Jimmy	113	-0.9	0.575	0.014	-0.230	0.105
A8-2	Jimmy	107.53	0.3	1.504	0.013	-1.321	0.089
A8-5	Jimmy	110.8	-0.7	0.472	0.016	-0.121	0.114
A8-4	Jimmy	109.75	-0.7	0.679	0.012	-0.487	0.132
N-28	Shavi	136.4	1.3	-0.107	0.018	0.005	0.092
N-27	Shavi	136.85	1.3	-0.159	0.011		
N-65	Shavi	137.75	-2.5	-0.735	0.018	1.327	0.114
N-24	Shavi	139.48	-5.7	-1.263	0.016	1.571	0.075
N-23	Shavi	140.5	-0.6	-0.889	0.018	1.435	0.144
N-21	Shavi	142.32	2.2	-1.512	0.019	1.648	0.061
N-18	SV	151.6	5.1	-0.735	0.024	0.685	0.177
N-17	SV	152	4.6	-0.769	0.013	0.723	0.284
N-16	SV	153.1	2.6	-0.898	0.036	0.726	0.115
N-13	SV	161	4.5	-0.112	0.016	0.342	0.131
N-84	SV	159.8	3.1	-0.012	0.037		
N-88	SV	162.1	3.1	-0.076	0.019	0.751	0.150
N-12	SV	162.9	1.2	-0.318	0.016	0.527	0.118
N-11	SV	164.46	4.0	-0.208	0.009	0.760	0.133
N-10	SV	166.63	2.4	-0.360	0.013	0.404	0.066

Table S-2 Mercury concentrations, total organic carbon (TOC; as reported in Yang *et al.*, 2019), calculated Hg/TOC, and Hg isotope data (in ‰) for the Manjeri Formation. Uncertainties (2σ) were 0.12 ‰ for δ^{202}Hg, 0.06 ‰ for Δ^{199}Hg, 0.05 ‰ for Δ^{200}Hg, and 0.08 ‰ for Δ^{201}Hg.

Sample	Member	Depth (m)	TOC (wt%)	Hg (ppb)	Hg/ TOC	δ^{202}Hg	Δ^{199}Hg	Δ^{200}Hg	Δ^{201}Hg
B1-1	Jimmy	61.5	0.8	165	198	-3.49	0.09	0.01	0.00
B2-1	Jimmy	63.31	0.5	122	239	-4.18	0.11	0.04	0.08
B2-3	Jimmy	65.2	0.7	48	65	-3.57	0.10	-0.01	0.04
B2-11	Jimmy	65.35		25		-2.20	0.10	-0.02	0.06
B2-15	Jimmy	67.06		14		-1.06	0.11	0.04	0.04
B2-18	Jimmy	68.14		25		-2.56	0.14	0.02	0.10
B2-20	Jimmy	69.16		29		-0.97	0.01	-0.02	0.04
B3-02	Jimmy	70.72	0.3	47	142	-3.73	0.10	0.01	0.05
B3-03	Jimmy	71.75	0.5	42	89	-3.39	0.05	0.00	0.02
B3-13	Jimmy	72.5		18		-2.47	0.05	-0.03	0.01
B3-14	Jimmy	73.15		12		-0.40	0.08	0.02	0.08
B3-17	Jimmy	74.74		11		-0.47	0.11	0.01	0.04
B4-19	Jimmy	75.58		10		-1.12	0.10	-0.01	0.02
B4-9	Jimmy	77.53		17		-3.03	0.15	-0.02	0.03
B4-12	Jimmy	79.35		3		-2.64	0.14	0.07	0.08
B4-15	Jimmy	80.65		12		-1.85	0.11	0.08	0.03
B4-07	Jimmy	83.1	0.4	55	148	-4.01	0.07	-0.02	0.01
B4-20	Jimmy	83.32		4		-1.51	0.02	-0.01	0.02
B4-08	Jimmy	84.13	0.4	12	32	-2.92	0.07	0.04	0.05
A7-6	Jimmy	102.65	0.8	10	13	-1.64	0.14	0.06	0.08
A7-7	Jimmy	103		12		-1.69	0.15	0.05	0.07
A7-8	Jimmy	103.85	0.6	9	15	-0.90	0.07	0.03	0.01
A7-3	Jimmy	104.48	0.6	31	49	-3.74	0.16	0.03	0.07
A7-4	Jimmy	105.53	0.5	24	45	-3.79	0.16	0.07	0.13
A8-2	Jimmy	107.53	0.5	157	310	-4.16	0.13	0.02	0.06
A8-3	Jimmy	108.58		22		-4.15	0.11	-0.02	0.04
A8-4	Jimmy	109.75	0.3	30	96	-3.16	0.08	0.01	0.04
A8-14	Jimmy	110.41		11		-1.29	0.09	0.01	0.05
A8-5	Jimmy	110.8	0.2	26	147	-3.43	0.11	0.03	0.06
A8-16	Jimmy	113		17		-1.70	0.08	0.06	0.07
N-28	Shavi	136.4	1.4	2066	1455	0.63	-0.05	0.01	-0.06
N-27	Shavi	136.85	1.3	2050	1627	1.02	-0.09	0.01	-0.12
N-65	Shavi	137.75		962		0.90	-0.07	-0.01	-0.05
N-24	Shavi	139.48	0.7	585	790	0.24	-0.02	0.00	-0.04
N-23	Shavi	140.5		1586		-0.11	-0.12	-0.02	-0.12
N-21	Shavi	142.32	0.7	1026	1487	-0.26	0.02	0.02	-0.03
N-18	SV	151.6	0.5	505	1075	0.55	-0.06	-0.01	-0.09
N-17	SV	152		492		-0.05	0.04	0.04	-0.02
N-16	SV	153.1		475		-0.88	0.02	0.02	0.00
N-84	SV	159.8		418		-0.97	0.05	0.03	0.00
N-13	SV	161	0.2	172	781	-1.14	0.03	-0.01	0.02
N-88	SV	162.1		99		-0.33	0.03	0.01	-0.02
N-12	SV	162.9	0.2	66	388	-0.38	0.02	0.02	0.02
N-11	SV	164.46	0.2	271	1503	-1.83	0.06	0.04	0.06
N-10	SV	166.63	0.2	447	2355	-0.26	-0.03	0.00	-0.04

Table S-3 Hg isotope values (in ‰) of NIST-3177 and GSS-4.

	THg (ng/mL)	δ^{202}Hg	δ^{202}Hg	δ^{202}Hg	δ^{202}Hg	Δ^{199}Hg	Δ^{200}Hg
3177-1	0.5	-0.14	-0.26	-0.35	-0.55	-0.01	0.01
3177-2	0.5	-0.11	-0.29	-0.47	-0.61	0.04	0.02
3177-3	0.5	-0.18	-0.33	-0.44	-0.57	-0.04	-0.04
3177-4	0.5	-0.13	-0.23	-0.39	-0.46	-0.01	0
3177-5	0.5	-0.14	-0.29	-0.48	-0.58	0.01	0
3177-6	0.5	-0.11	-0.2	-0.36	-0.48	0.02	0.04
3177-7	0.5	-0.17	-0.26	-0.42	-0.5	-0.04	-0.01
3177-8	0.5	-0.1	-0.25	-0.42	-0.47	0.01	-0.02
Average		**-0.14**	**-0.26**	**-0.42**	**-0.53**	**0**	**0**
2SD		**0.06**	**0.08**	**0.1**	**0.12**	**0.06**	**0.05**
GSS-4-1	0.5	-0.8	-0.79	-1.61	-1.69	-0.38	0.02
GSS-4-2	0.5	-0.87	-0.87	-1.68	-1.77	-0.43	-0.02
GSS-4-3	0.5	-0.82	-0.8	-1.64	-1.69	-0.39	0.03
Average		**-0.83**	**-0.82**	**-1.65**	**-1.72**	**-0.4**	**0.01**
2SD		**0.07**	**0.08**	**0.08**	**0.09**	**0.05**	**0.05**

Supplementary Figures

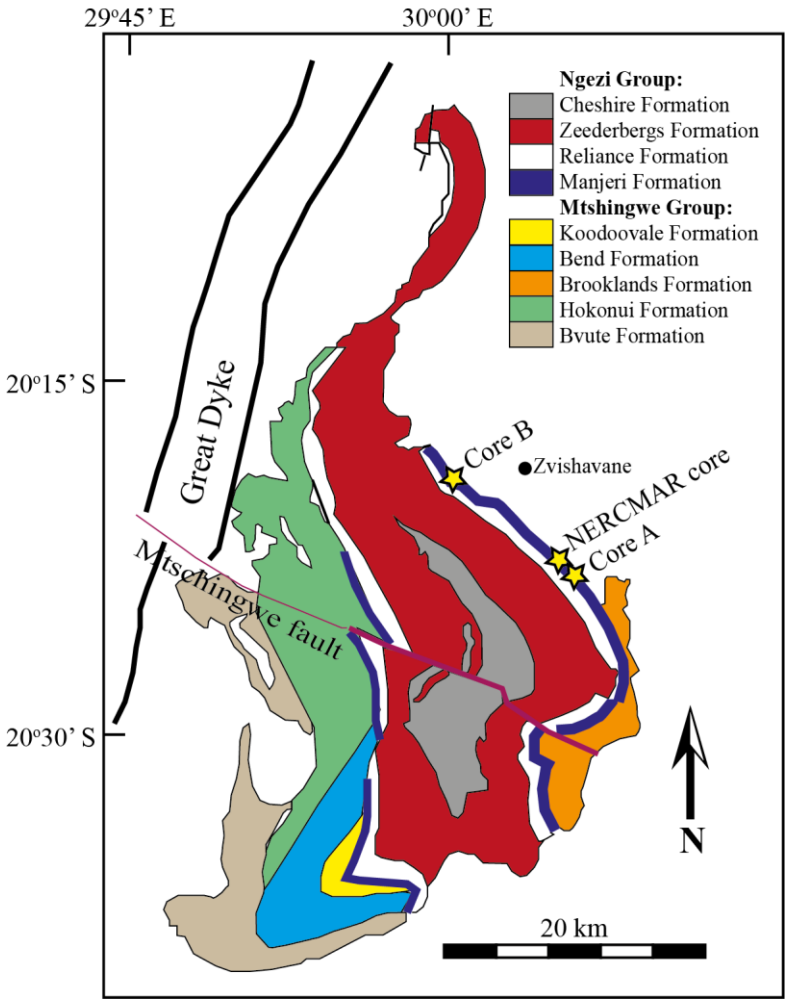

Figure S-1 Simplified geological map of the Belingwe Greenstone Belt, showing locations of the NERCMAR core, Core A and Core B (modified from Thomazo *et al.*, 2013).

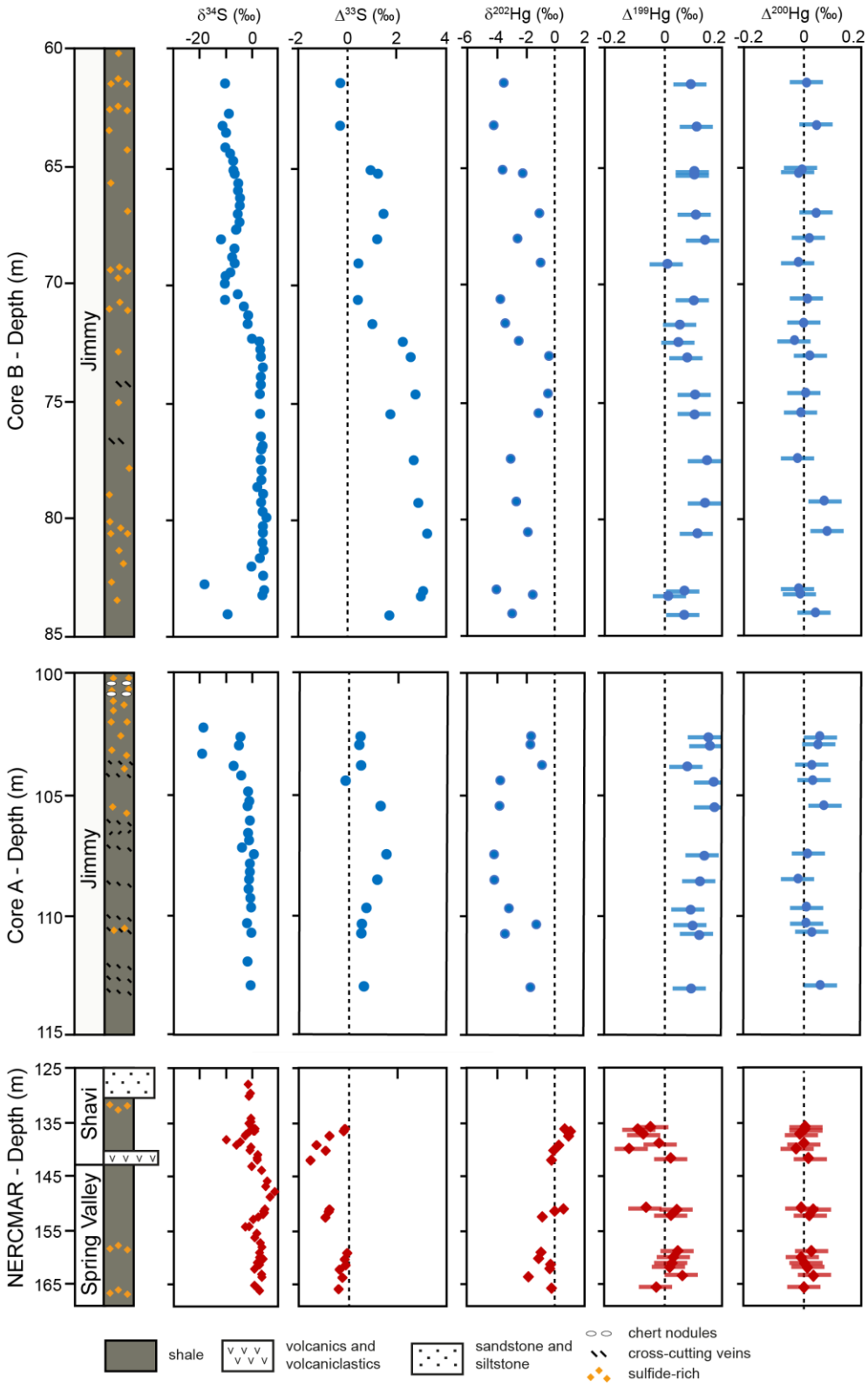

Figure S-2 Sulfur and mercury isotope data, plotted alongside core stratigraphy. Details of stratigraphic units and $\delta^{34}S$ data were previously reported in Yang *et al.* (2019).

Supplementary Information References

Bergquist, B.A., Blum, J.D. (2007) Mass-dependent and -independent fractionation of Hg isotopes by photoreduction in aquatic systems. *Science* 318, 417-420.

Blum, J.D., Bergquist, B.A. (2007) Reporting of variations in the natural isotopic composition of mercury *Analytical and Bioanalytical Chemistry* 388, 353-359.

Bolhar, R., Hofmann, A., Woodhead, J., Hergt, J., Dirks, P. (2002) Pb- and Nd-isotope systematics of stromatolitic limestones from the 2.7 Ga Ngezi Group of the Belingwe Greenstone Belt: constraints on timing of deposition and provenance. *Precambrian Research* 114, 277-294.

Deng, C., Sun, G., Rong, Y., Sun, R., Sun, D., Lehmann, B., Yin, R. (2021) Recycling of mercury from the atmosphere-ocean system into volcanic-arc-associated epithermal gold systems. *Geology* 49, 309-313.

Grassineau, N.V., Abell, P., Appel, P.W.U., Lowry, D., Nisbet, E.G. (2006) Early life signatures in sulfur and carbon isotopes from Isua, Barberton, Wabigoon (Steep Rock) and Belingwe Greenstone Belts (3.8 to 2.7 Ga). *Geological Society of America Memoirs* 198, 33-52.

Izon, G., Zerkle, A.L., Zhelezinskaia, I., Farquhar, J., Newton, R.J., Poulton, S.W., Eigenbrode, J.L., Claire, M.W. (2015) Multiple oscillations in Neoarchean atmospheric chemistry. *Earth and Planetary Science Letters* 431, 264-273.

Nisbet, E.G., Arndt, N.T., Bickle, M.J., Cameron, W.E., Chauvel, C., Cheadle, M., Hegner, E., Kyser, T.K., Martin, A., Renner, R., Roedder, E. (1987) Uniquely fresh 2.7 Ga komatiites from the Belingwe greenstone belt, Zimbabwe. *Geology* 15, 1147-1150.

Thomazo, C., Grassineau, N.V., Nisbet, E.G., Peters, M., Strauss, H. (2013) Multiple sulfur and carbon isotope composition of sediments from the Belingwe Greenstone Belt (Zimbabwe): A biogenic methane regulation on mass independent fractionation of sulfur during the Neoarchean? *Geochimica et Cosmochimica Acta* 121, 120-138.

Warke, M.R., Di Rocco, T., Zerkle, A.L., Lepland, A., Prave, A.R., Martin, A., Ueno, Y., Condon, D.J., Claire, M. (2020) The Great Oxidation Event preceded a Paleoproterozoic "snowball Earth". *PNAS* 117, 13314-13320.

Yang, J., Junium, C.K., Grassineau, N.V., Nisbet, E.G., Izon, G., Mettam, C., Martin, A., Zerkle, A.L. (2019) Ammonium availability in the Late Archaean nitrogen cycle. *Nature Geoscience* 12, 553-557.

Yin, R., Krabbenhoft, D.P., Bergquist, B.A., al., e. (2016) Effects of mercury and thallium concentrations on high precision determination of mercury isotopic composition by Neptune Plus multiple collector inductively coupled plasma mass spectrometry. *Journal of Analytical Atomic Spectrometery* 31, 2060-2068.